

# FLUX RATIOS AS A PROBE OF DARK SUBSTRUCTURES IN QUADRUPLE-IMAGE GRAVITATIONAL LENSES

R. BENTON METCALF<sup>1</sup> & HONGSHENG ZHAO<sup>1</sup>  
 Institute of Astronomy, Cambridge, CB3 0HA, UK  
*Draft version October 27, 2018*

## ABSTRACT

We demonstrate that the flux ratios of 4-image lensed quasars provide a powerful means of probing the small scale structure of Dark Matter (DM) halos. A family of smooth lens models can precisely predict certain combinations of flux ratios using only the positions of the images and lens as inputs. Using 5 observed lens systems we show that real galaxies *cannot* be described by smooth singular isothermal ellipsoids, nor by the more general elliptical power-law potentials. Large scale distortions from the elliptical models can not yet be ruled out. Nevertheless we find, by comparing with simulations, that the data can be accounted for by a significant ( $\geq 5 - 10\%$ ) amount of dark substructures within a projected distance of several kpc from the center of lenses. This interpretation favors the Cold Dark Matter (CDM) model over the warm or self-interacting DM models.

*Subject headings:* cosmology: theory — dark matter — galaxies: formation — gravitational lensing

## 1. INTRODUCTION

The standard  $\Lambda$ CDM cosmological model has been very successful in accounting for observations on scales larger than around a Mpc. But mounting evidence points towards difficulties for this theory on the scales of galaxies and dwarf galaxies (van den Bosch *et al.* 2000; Gnedin & Zhao 2001). Most interestingly for this paper, CDM simulations of the local group of galaxies predict an order of magnitude more dwarf galaxy halos with masses greater than  $\sim 10^8 M_{\odot}$  than there are observed satellites of the Milky Way (MW) Galaxy and the M31 galaxy (Moore *et al.* 1999; Klypin *et al.* 1999; Mateo 1998).

This overprediction of dwarf halos could be a sign that there is something fundamentally wrong with the CDM model – the variants include warm dark matter (e.g., Bode, Ostriker & Turok 2001), self-interacting dark matter (Spergel & Steinhardt 2000) and unorthodox inflation models (Kamionkowski & Liddle 2000). Alternatively, the small DM clumps could exist, but not contain stars, so as to escape detection as observable dwarf galaxies. This situation can easily, perhaps inevitably, come about through the action of feedback processes in the early universe (photoionization and supernova winds) (e.g., Somerville 2001). Several authors, e.g. Metcalf (2001), have argue that the overabundance of DM clumps is likely to extend down to smaller masses and larger fractions of the halo mass than have thus far been accessible to numerical simulations. These nearly pure dark matter structures have largely been considered undetectable.

Metcalf & Madau (2001) showed that if the CDM model is correct and these substructures exist within the strong gravitational lenses responsible for multiply imaged QSOs they will have a dramatic effect on the image magnifications – compound gravitational lensing. It was proposed that the image positions which are only weakly affected by substructure could be used to constrain a smooth model for the lens. The magnification ratios can then be compared with the predictions of this model. However, to

detect this effect the model or family of models must accurately predict the magnification ratios at around the  $\sim 0.1$  mag level. It must be certain that there is no smooth lens model which can reproduce both the observed ratios and image positions. This is the task that is taken up in this paper.

Mao & Schnieder (1998) first proposed that the magnification ratios of B1422+231 are better fit by a model with substructure in it than with a smooth model. They fixed the smooth model and added point masses to represent globular clusters and plane wave perturbations. They found that they could reproduce the ratios with small scale fluctuations of relatively large amplitude. This does not however explain the discrepancies between radio and optical ratios in this system. Recently Chiba (2001) has done a similar analysis where the smooth model is fixed and masses are added. He concludes that globular clusters and dwarf galaxies (as represented by point masses) are not sufficient to reproduce the data. Both these investigations were restricted to the singular isothermal ellipsoidal models for the lens galaxy, an assumption which we do not make here. During the refereeing process of this paper a few other preprints appeared on very similar topics (Dalal & Kochanek 2001, Keeton 2001 and Bradač *et al.* 2001).

## 2. METHOD

### 2.1. The Lens model

The lensing equation,  $\vec{z} = \vec{x} - \vec{\alpha}(\vec{x})$ , relates a point on the source plane  $\vec{z}$  to a point on the image plain  $\vec{x}$ , where  $\vec{\alpha}(\vec{x})$  is the deflection angle. These are angular positions. The deflection angle can be expressed as the gradient of a lensing potential:  $\vec{\alpha}(\vec{x}) = \vec{\nabla}\psi(\vec{x})$ . This potential is related to the surface density of the lens,  $\Sigma(\vec{x})$ , through the two dimensional Poisson equation

$$\nabla^2\psi(\vec{x}) = 2\kappa(\vec{x}) \quad , \quad \kappa(\vec{x}) = \Sigma(\vec{x})/\Sigma_c. \quad (1)$$

where  $\Sigma_c \equiv c^2 D_s (4\pi G D_l D_{ls})^{-1}$  is the critical surface density. Here  $D_l$ ,  $D_s$ , and  $D_{ls}$  are the angular size distances

<sup>1</sup> Email: bmetcalf@ast.cam.ac.uk, zhao@ast.cam.ac.uk

to the lens, source, and from the lens to the source, respectively.

To model the lens galaxy we use an elliptical potential with a power-law radial profile (EPL). The influence of other galaxies that might neighbor the primary lens is included through a background shear (EPL+S). The potential for these models is

$$\psi(x, y) = br_\epsilon^{2n} + \frac{1}{2}\gamma [(\Delta x^2 - \Delta y^2) \cos 2\theta_\gamma + 2\Delta x \Delta y \sin 2\theta_\gamma] \quad (2)$$

$$\begin{aligned} \Delta x &\equiv (x - x_l) \quad , \quad \Delta y \equiv (y - y_l) \\ r_\epsilon^2 &\equiv \Delta x^2 (\cos^2 \theta_\epsilon + \epsilon^2 \sin^2 \theta_\epsilon) \\ &\quad + \Delta y^2 (\sin^2 \theta_\epsilon + \epsilon^2 \cos^2 \theta_\epsilon) \\ &\quad + \Delta x \Delta y (1 - \epsilon^2) \sin 2\theta_\epsilon \end{aligned} \quad (3)$$

where the center of the lens is located at  $\vec{x}_l = (x_l, y_l)$ . The second term in the potential (2) is the external shear. With the addition of the source position the number of free parameters comes to 10. A singular isothermal sphere corresponds to  $n = 0.5$  and  $\epsilon = 1$  and a point mass would be indicated if  $n$  were close to zero (in this case  $\psi \propto \ln r$ ).

### 2.2. Searching parameter space

Typically the lens model and thus the likelihood are functions of many parameters – in our case 10. As a result characterizing the properties of a family of models in any more detail than simply finding the best fitting set of parameters can be difficult. Most, perhaps all, authors have taken a Monte Carlo approach where the image positions are chosen at random according to the observational uncertainties. Then the best-fit model is found and the parameters of that model are recorded. This is *not* the correct procedure. There is not generally a one-to-one correspondence between image positions and model parameters; not all sets of image positions correspond exactly to a set of model parameters. The region over which one can legally vary the positions is highly restricted (in 10 dimensions). In addition, if the model has a high degree of freedom multiple sets of parameters may correspond to the same image positions.

To avoid these problems we generate random models and then calculate the image positions. This is significantly more time consuming because one does not know how well a parameter set fits the data until all the calculations are finished. To achieve any degree of efficiency and to ferret out the corners of confidence regions some adaptive sampling of the parameters must be used. We do this by first finding the best-fit model and set a maximum  $\chi^2$  that we consider an acceptable fit. The models are chosen according to the probability  $P(\mathbf{x}) = \prod_i p(x_i, \sigma_i)$  where each  $p(x_i, \sigma_i)$  is a normal distribution. The parameters  $x_i$  are the distance from the best-fit model along each of the principle directions of the distribution of models already found in the acceptable-fit region. These directions are periodically updated. The standard deviations  $\sigma_i$  are updated so that it is some fixed factor times the distance to most extreme acceptable-fit model in that direction. This factor is increased until the final confidence region is no longer dependent on it, typically  $\sim \sqrt{3}$ . This algorithm works well except when the acceptable-fit region is highly

curved in parameter space or has long thin regions projecting from a thicker region. The most difficult task is to find the boundaries of the very high confidence regions. As a result the 95% confidence intervals reported here are more secure than the 99% ones although we do believe that the calculation has converged in all cases.

In this paper we are primarily interested in the magnification ratios. For a 4-image system we can combine the fluxes into three independent quantities of the form

$$q^j = \sum_{i=1}^4 a_i^j m^i \quad ; \quad \sum_{i=1}^4 a_i^j = 0 \quad (4)$$

where  $m^i$  is the magnitude of the  $i$ th image. The constraint on  $a_i^j$  ensures that  $q^j$  is independent of the source luminosity. In addition we require that the transformation from the observed magnitudes be orthogonal so that the  $q^i$ 's are still measured in magnitudes. We choose three orthogonal generalized flux ratios such that one of them has the smallest confidence interval and one of them has the largest. This displays the maximum precision to which the magnification ratios can be predicted.

### 3. DATA

We model five 4-image systems (MG0414+0534, B1422+231, PG1115+080, Q2237+030 and H1413+117) using publicly available data. For the positions of the QSO images and the center of the lens galaxy we use HST data available on the CASTLES Survey's web site (<http://cfa-www.harvard.edu/castles/>). We use the infrared and visible extinction-corrected flux ratios from Falco *et al.* (1999). The errors in the IR/visible ratios are dominated by uncertainties in the extinction correction rather than photometric errors. The radio data comes from Katz, Moore & Hewitt (1997) for MG0414, from Patnaik *et al.* (1992) for B1422, and from Falco *et al.* (1996) for Q2237.

### 4. RESULTS

In Table 1 some of the best-fit lens parameters for the five 4-image systems are given along with the coefficients for the generalized magnification ratio. It should be noted that in practice the likelihood is often rather flat in some directions near the maximum as is most clearly the case in MG0414 (see figure 1). Our Monte Carlo technique tries to account for these difficulties. In addition there can also be local maxima that are well separated in parameter space. For B1422 we find two well fitting regions of parameter space. They do not appear to be connected at any reasonable confidence level. In every case the best-fit model fits the image and lens positions very well which is expected since we have an equal number of constraints and parameters. The image positions are all consistent with the hypothesis that the EPL+S models correctly describe the lens potentials.

Figure 1 shows the magnification ratio confidence regions along with the data. The generalized magnification ratios have been shifted for convenience so that the confidence region is centered on zero magnitudes in all cases except B1422 where we have two acceptable-fit regions. Here the ratios are shifted so that the region with the globally best fitting solution is centered on 0. It is significant that the width 99% confidence interval for the best

generalized ratio is  $< 0.06$  mag in all cases except MG0414 where it is 1.1 mag. The data is also plotted in figure 1 with the size of the symbols representing the errors transformed into the generalized ratios. One can immediately see that many of the measurements are inconsistent with the smooth EPL+S model. Only MG0414 is fully consistent with the models. Of the two acceptable regions for B1422 it is the one that fits the image positions less well that fits the flux ratios best.

## 5. LENSING SIMULATIONS

For comparison we have done some simulations of what is expected in the CDM model. We have not attempted to account for the fact that the image positions do not constrain the smooth model to a precise set of smooth model parameters. Because the effects of substructure are strongly dependent on the smooth model used only a qualitative comparison with the CDM model is now possible. We will make a more systematic study of this problem in future work.

The code used to do these simulations is described in Metcalf & Madau (2001). The smooth models are fixed to the best fit models given in Table 1. The substructure is modeled as singular isothermal spheres cut off at the tidal radius. The mass function is  $\propto m^{-2}$  between  $10^4 M_\odot$  and  $10^6 M_\odot$  and the normalization is fixed so that 5% and 10% of the lens surface density is contained in the substructure. The physical radius of the sources are set to 30 pc which is perhaps appropriate for the radio emission. We calculate 1500 random realization of the ratios for each lens. We did not simulate H1413 because the lens redshift is not known

The results are shown in figure 2. Except for the second ratio of Q2237, all of the anomalous ratios fall within  $2\sigma$  of the regions containing 95% of the simulated ratios if 10% of the mass is put in substructure. If anything the data appears to favor even more substructure or higher mass substructure relative to the source size.

## 6. DISCUSSION

In all cases except MG0414 the EPL+S models are ruled out at greater than 95% confidence. The radio fluxes are not affected by extinction or microlensing and they alone rule out the models for B1422 and Q2237. The disagreement between visible and radio ratios in Q2237 is confirmation of the microlensing that was already known to exist through time variability studies (Woźniak *et al.* 2000, and references there in). The strong disagreement between the radio and model predictions for Q2237 does indicate that there is some other kind of substructure there as well. Given the absence of microlensing-related strong variability in PG1115 or H1413 the observed visible/IR flux ratios appear inconsistent with EPL+S models. This is evidence that a significant amount of small scale structure must exist either in the lenses or along the lines of sight.

The known populations of small scale substructures in the Galaxy would be unlikely to cause the effects reported here. The overdensities in spiral arms do not appear large enough and, as pointed out by Mao & Schneider (1998), the fraction of the Galaxy halo's mass in globular clusters is only about  $\sim 10^{-4}$ . The mass in dwarf galaxy satellites is  $\sim 1\%$  of the halo, but 80 – 90% of this is in just two objects. One would expect a chance alignment of these types of structures with the QSO images to be rare not ubiquitous.

Within the EPL+S models the magnification ratios are quite strongly constrained in some dimensions. In all but MG0414 we were able to constrain one combination of magnification ratios to within 0.06 mag. Within a large family of galactic mass profiles the ratios can be an effective tool for probing small scale structure. In simulations with pure CDM, galaxies do have power-law radial profiles within the small radial distances important for quad-lenses. And observed lens galaxies are typically relaxed giant ellipticals. However, there is no compelling reason to believe that CDM halos and their embedded galaxies should be precisely elliptical; bulges and inclined disks could make the lens mass distribution more boxy or more disky in projection in the inner few kpc. Zhao & Pronk (2001) have found that lens models with different degrees of boxiness can fit the image positions equally well, but predict different flux ratios and time delay ratios. This leads to an ambiguity in our substructure interpretation with large scale distortion. Ultimately this degeneracy can be lifted by either restricting the range of realistic halo profiles using simulations or by comparing observations in different wavelengths – the magnifications should be wavelength dependent (Metcalf & Madau 2001).

The constraints on the predicted magnification ratios are good, but they are not negligible. In some cases the uncertainty in the ratios is much larger than the expected variations caused by substructure. The influence of substructure on the ratios can be strongly dependent on the precise values of smooth model parameters. This should be taken into account in future compound lensing studies.

This result is in rough agreement with what is expected in the CDM model (Metcalf & Madau 2001) as shown by our simulations. In variants of the CDM model such as warm DM, hot DM or interacting DM small scale substructure is almost nonexistent. These models are not simultaneously consistent with the EPL+S lens models and the observed flux ratios. Possible degeneracies with the larger scale distortions of the lens make us unable to conclusively discriminate between DM models at present.

## Acknowledgements

RBM would like to thank Piero Madau for very useful conversations.

## REFERENCES

- Bode, P., Ostriker, J. P., & Turok, N. 2001, *ApJ*, 556, 93  
 Bradač, M., Schneider, P., Steinmetz, M., Lombardi, M., King, L.J., & Porcas, R., 2001, preprint, astro-ph/0112038  
 Chiba, M. 2001, *ApJ*, in press, (astro-ph/0109499)  
 Dalal, N. & Kochanek, C., 2001, preprint, astro-ph/0111456  
 Falco, E.E., Impey, C.D., Kochanek, C.S., Lehár, J., McLeod, B.A., Rix, H., Keeton, C.R., Muñoz, J.A. & Peng, C.Y., 1999, *ApJ*, 523, 617.  
 Falco, E.E., Lehar, J., Perley, R.A., Wambsganss, J. & Gorenstein, M.V., 1996, *AJ*, 112, 897  
 Gnedin, O. & Zhao, H., 2001, submitted to MNRAS, (astro-ph/0108108)

- Keeton, C.R., 2001, preprint, astro-ph/0111595  
Kamionkowski, M. & Liddle, A., 2000, Phys. Rev. Lett., 84, 4525  
Katz, C.A., Moore, C.B. & Hewitt, J.N., 1997, ApJ, 475, 512  
Klypin, A., Kravtsov, A.V., Valenzuela, O., & Prada, F. 1999, ApJ, 522, 82  
Mao, S., & Schneider, P. 1998, MNRAS, 295, 587  
Mateo, M. 1998, ARA&A, 36, 435  
Metcalf, R.B., 2001, "Where is the Matter?", ed. Tresse, L. & Treyer, M., (astro-ph/0109347)  
Metcalf, R.B. & Madau, P., 2001, ApJ in press, (astro-ph/0108224)  
Moore, B., Ghigna, S., Governato, F., Lake, G., Quinn, T., Stadel, J., & Tozzi, P. 1999, ApJ, 524, L19  
Patnaik, A.R., Browne, I.W.A., Walsh, D., Chaffee, F.H. & Foltz, C.B., 1992, MNRAS, 259, 1P  
Somerville, R. S., 2001, submitted to ApJ (astro-ph/0107507)  
Spergel D. N., Steinhardt P. J., 2000, Phys. Rev. Lett., 84, 3760  
van den Bosch F. C., Robertson B. E., Dalcanton J. J., de Blok W. J. G., 2000, AJ, 119, 1579  
Woźniak, P.R., Alard, C., Udalski, A., Szymański, M., Kubiak, M., Pietrzyński, G. & Żebruń, K., 2000, ApJ, 529, 88-92.  
Zhao, H. & Pronk, D., 2001, MNRAS, 320, 402

Lens	Best-Fit Lens Models					Generalized Ratios		
	$P(\chi^2)$	$b$	$\gamma$	$\epsilon^2$	$n$	$a_1$	$a_2$	$a_3$
B1422+231	0.00	0.91	0.25	1.58	0.32	-0.61	0.76	-0.20
	0.00	2.00	0.36	2.38	0.11	0.61	0.62	0.49
PG1115+080	0.00	14.7	0.21	1.13	0.04	-0.73	0.69	-0.03
	0.00	1.44	0.05	1.37	0.28	0.61	0.62	0.49
Q2237+030	0.00	1.44	0.05	1.37	0.28	-0.76	0.65	0.08
	0.00	1.44	0.05	1.37	0.28	0.65	0.76	0.05
H1413+117	0.21	0.45	0.10	1.21	0.97	0.77	0.01	-0.63
	0.21	0.45	0.10	1.21	0.97	-0.56	-0.45	-0.69
MG0414+0534	0.00	0.10	0.85	0.52	0.65	-0.63	0.57	0.52
	0.00	0.10	0.85	0.52	0.65	0.77	0.48	0.41
						-0.004	-0.01	-0.999
						-0.68	-0.73	0.01

TABLE 1

THE  $a_i$  COEFFICIENTS ARE FOR THE MOST WELL CONSTRAINED GENERALIZED MAGNIFICATION RATIO ON TOP AND THE LEAST WELL CONSTRAINED RATIO ON THE BOTTOM ( $a_4 = -\sum_{i=1}^3 a_i$ ). THE THIRD GENERALIZED RATIO IS ORTHOGONAL TO THESE TWO VECTORS. THE NUMBERING OF IMAGES IS IN THE SAME ORDER AS THOSE IN THE OBSERVATIONAL LITERATURE.  $P(\chi^2)$  IS THE EXPECTED PROBABILITY (ROUNDED OFF) OF  $\chi^2$  BEING SMALLER THAN THE ONE MEASURED WITH 10 DEGREES OF FREEDOM. OF THE TWO MODELS FOR B1422 THE SECOND ONE IS A SLIGHTLY BETTER FIT TO THE IMAGE POSITIONS.

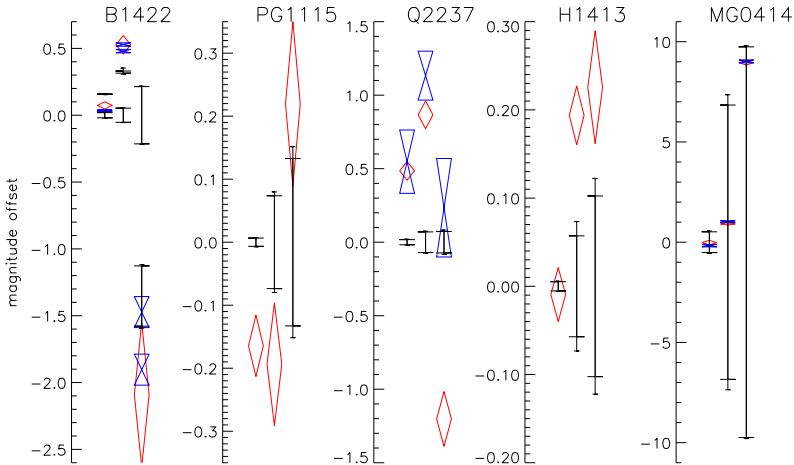


FIG. 1.— The confidence ranges for the EPL+S in the optimal three independent combinations of the magnification ratios for five lens systems. The 95% and 99% confidence regions are shown by the two sets of horizontal bars on each error bar. The bow ties mark the radio ratios at 5 GHz except for B1422 where both 5 GHz and 8 GHz ratios are shown. The size of the bow ties are the reported errors. The diamonds mark the extinction-corrected infrared and visible ratios with the lengths giving the errors (Falco *et al.* 1999).

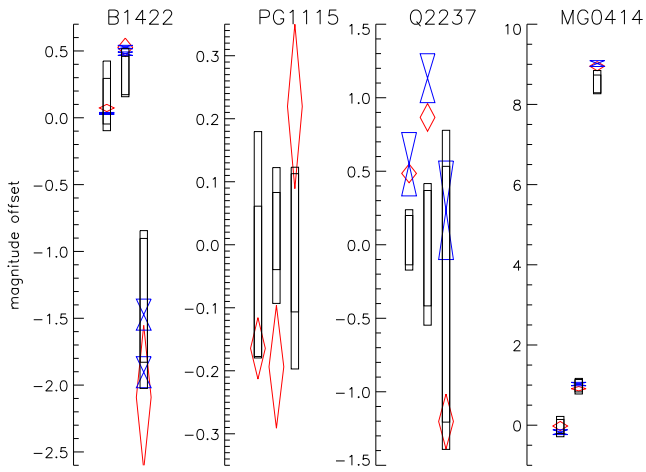


FIG. 2.— Same as figure 1 except that the smooth models are fixed and the range of magnification ratios expected in the presence of substructure are shown as rectangles. The rectangles show the region in which 95% of the simulated realizations fall. There are two rectangles for each ratio, one inside the other. The smaller ones are for the case of 5% of the surface density in substructure and the larger ones are for 10%. The scale has been changed from figure 1 for MG0414 for clarity.